Local Positive Feedback by Calcium in the Propagation of Intracellular Calcium Waves*

Samuel S.-H. Wang and Stuart H. Thompson
Neurosciences Program and Hopkins Marine Station of Stanford University, Pacific Grove, California 93950 USA

ABSTRACT In many types of eukaryotic cells, the activation of surface receptors leads to the production of inositol 1,4,5-trisphosphate and calcium release from intracellular stores. Calcium release can occur in complex spatial patterns, including waves of release that traverse the cytoplasm. Fluorescence video microscopy was used to view calcium waves in single mouse neuroblastoma cells. The propagation of calcium waves was slowed by buffers that bind calcium quickly, such as BAPTA, but not by a buffer with slower on-rate, EGTA. This shows that a key feedback event in wave propagation is rapid diffusion of calcium occurring locally on a scale of <1 μm. The length-speed product of wavefronts was used to determine that calcium acting in feedback diffuses at nearly the rate expected for free diffusion in aqueous solution. In cytoplasm, which contains immobile Ca^{2+} buffers, this rate of diffusion occurs only in the first 0.2 ms after release, within 0.4 μm of a Ca^{2+} release channel mouth. Calcium diffusion from an open channel to neighboring release sites is, therefore, a rate-determining regenerative step in calcium wave propagation. The theoretical limitations of the wave front analysis are discussed.

INTRODUCTION

The stimulation of surface receptors leads to release of ionized calcium, Ca^{2+}, from internal stores in many cell types (Berridge, 1993). Ca^{2+} release, which comes from stores in the endoplasmic reticulum, is a signal that often takes the form of a wave that crosses the cell and spreads to every region (Gilkey et al., 1978). These propagating calcium signals are thought to have functional significance in establishing polarity in eggs at fertilization (Gilkey et al., 1978), coordinating ciliary beating in airway epithelia (Boitano et al., 1992), and directing fluid secretion across epithelial cells (Kasai and Augustine, 1990).

Calcium waves propagate quickly and without slowing, ruling out purely passive diffusion of calcium as the underlying cause. The mechanism is instead an active one involving local re-excitation. This enables the signal to travel much farther than it could by diffusion alone, and waves of second messenger generation have been suggested to be a means of carrying chemical signals over long distances (Winfree, 1987).

Active wave propagation requires a positive feedback step in which newly generated messenger diffuses to a neighboring region and causes the generation of more messenger. The speed of a spreading wave in such a reaction-diffusion system is limited in part by the rate of diffusion of the feedback messenger. Knowing the identity of the feedback messenger is therefore essential to a full understanding of wave propagation. In the case of agonist-evoked calcium waves, there are two candidates for the rate-limiting factor: the second messenger that binds to receptors to cause calcium release, inositol-1,4,5-trisphosphate (IP_3), and calcium itself.

IP_3 is formed by receptor-activated phospholipase C and stimulates receptors in the endoplasmic reticulum to release Ca^{2+}. The activity of phospholipase C is enhanced by the action of micromolar Ca^{2+} (Renard et al., 1987; Rhee et al., 1989). If production of IP_3 were stimulated locally by the release of calcium, diffusion of IP_3 to neighboring release sites could cause further release and, therefore, wave propagation. Because the dose-response curve of IP_3 action on its receptor has a steep rising phase, with at least threefold positive apparent cooperativity (Meyer et al., 1988; Parker and Ivorra, 1990), even a shallow wave of IP_3 might be rate-limiting in the generation of a calcium wave.

On the other hand, it has been suggested that released calcium is the rate-limiting diffusible factor (Jaffe, 1983; Backx et al., 1989; Lechleiter et al., 1991; DeLisle and Welsh, 1992). This is suggested by the observation that Ca^{2+} acts positively on the IP_3 receptor to increase opening probability and cause further Ca^{2+} release. This occurs rapidly, within a fraction of a second, when calcium rises to micromolar concentrations (Iino, 1990; Bezprozvanny et al., 1991; Finch et al., 1991). Local feedback could therefore take place in the domain surrounding an open IP_3 channel mouth, where calcium rises to micromolar levels (Smith and Augustine, 1988; Stern, 1992).

To investigate the positive feedback role of Ca^{2+} in wave propagation, we tested the idea that Ca^{2+} ions emanating from open IP_3 receptor channels provide the necessary re-excitation by diffusing to other channels. If this mechanism applies, it

Received for publication 17 March 1995 and in final form 27 July 1995.
Address reprint requests to Dr. Samuel S.-H. Wang, Box 3209, Department of Neurobiology, Duke University Medical Center, Durham, NC 27710. Tel.: 919-681-6165; Fax: 919-684-4431; E-mail: abba@neuro.duke.edu. Dr. Thompson: Tel.: 408-655-6223; Fax: 408-375-0793; E-mail: stuartt@leland.stanford.edu.

This article contains an electronic supplement on the topic of calcium diffusion into a nonsaturable buffer. This work, which was an Appendix to the first author's doctoral dissertation, is available as Tex and SigmaPlot files. These files can be found on the Biophysical Journal ftp server under BJ_Supplements/Ca-Ca_Waves. Please see the Biophysics on the Internet page at the end of this issue for instructions for accessing this information.

0006-3495/95/11/1683/00 $2.00

should be possible to modify parameters of wave propagation by adding exogenous Ca^{2+} buffers. We show that exogenous Ca^{2+} buffers slow wave propagation provided that the buffer has a rapid on-rate. This establishes the fact that locally diffusing Ca^{2+} plays a role in wave propagation.

Based on theoretical considerations, measurements of wave properties were then used to estimate the spatial and temporal range over which Ca^{2+} works in feedback. Images of waves were analyzed to obtain values of the length-speed product ($L \cdot v$) of the advancing wave front. Reaction-diffusion theory states that $L \cdot v$, which has the units of a diffusion constant, gives the diffusion constant of the feedback messenger. However, Ca^{2+} does not diffuse at a constant rate in cytoplasm. After Ca^{2+} ions emerge from an IP_3 receptor channel, their movement in the cytosol is slowed by binding to less mobile buffer molecules, and the diffusion "constant" of Ca^{2+} ions is therefore time dependent.

We defined an apparent diffusion constant, D_{app}, in terms of the mean-squared displacement of the total population of Ca^{2+} ions and calculated its time dependence under physiological buffering conditions. We then assumed that $L \cdot v$ gave the D_{app} of Ca^{2+} during the diffusion step preceding positive feedback. Given the properties of cytoplasmic Ca^{2+} buffers, this observed D_{app} is consistent with a step in which Ca^{2+} diffuses for less than 0.2 ms on average before causing further Ca^{2+} release. The average distance traversed by Ca^{2+} in that time is less than 0.4 μm. These calculations appear in the Appendix and in the Electronic Supplement.

This wave front analysis assumes an extension of existing theory to buffered systems. In an unbuffered calcium release system, the diffusion constant of the feedback messenger is $D > L \cdot v$. In the case of a buffer that is in constant equilibrium with the messenger, a simplified model with only one messenger suggests that this relation becomes $D_{app} > L \cdot v$, where D_{app} is the apparent diffusion constant of the messenger (Sneyd and Kalachev, 1994). However, our buffer-loading results show that feedback occurs before binding equilibrium takes place. Final interpretation of our wavefront observations awaits a rigorous theoretical analysis of this case.

We used the mouse neuroblastoma cell line N1E-115, which is well suited for the study of IP_3-mediated Ca^{2+} release waves. Like many eukaryotic cells, they have IP_3 production and Ca^{2+} release machinery (Surichamorn et al., 1990), and in these cells activation of muscarinic acetylcholine or histamine receptors leads to Ca^{2+} release (Oakes et al., 1988; Surichamorn et al., 1990; Wang and Thompson, 1994). During the first 30 s of agonist-evoked Ca^{2+} signaling, the increase in $[Ca^{2+}]_i$ is caused entirely by release from intracellular Ca^{2+} stores with no measurable contribution from influx (Mathes and Thompson, 1994). Also, N1E-115 cells do not exhibit calcium-induced calcium release (CICR) involving ryanodine receptors, because Ca^{2+} release is insensitive to ryanodine receptor blockers (Wang et al., 1995). Positive calcium feedback in these cells therefore takes place at IP_3 receptors.

MATERIALS AND METHODS

Cell culture

N1E-115 neuroblastoma cells were prepared as described previously (Wang and Thompson, 1994). For experiments, cells were plated on coverslips and grown to 60–80% confluence; at this time the medium was replaced with differentiation medium containing 2% dimethylsulfoxide (Kimhi et al., 1976). Cells were used 7–21 days after differentiation.

Drug applications

Carbachol and histamine solutions were applied by total, vigorous replacement of the chamber saline using a computer-controlled perfusion device. Six successive exchanges with normal saline at the end of the drug application ensured that no drug remained in the chamber, thus preventing receptor desensitization (Wang and Thompson, 1994). The external saline contained (mM): NaCl 137, KCl 5.4, $CaCl_2$ 1.8, $MgSO_4$ 0.8, KH_2PO_4 0.4, Na_2HPO_4 0.3, glucose 23, and NaHEPES 20 (pH 7.4, T = 27–30°C). A 15–30-min recovery period between agonist applications ensured the reproducibility of the response. High-potassium saline contained (mM): NaCl 5, KCl 140, $CaCl_2$ 1.8, $MgSO_4$ 0.8, glucose 23, and NaHEPES 20 (pH 7.4, T = 27–30°C).

Calcium imaging

Cells were loaded with the calcium indicator fura-2 (Grynkiewicz et al., 1985) by incubation in saline containing 5 μM fura-2/AM (Molecular Probes, Eugene, OR) and 0.025% Pluronic acid F-127 (Molecular Probes) for 60 min at 22°C. In wave-slowing experiments, loading with additional chelators was achieved by incubating cells with AM ester while they were on the microscope stage. After each loading, at least 15 min was allowed for the cell to re-equilibrate Ca^{2+} levels.

Fluorescence imaging was performed on a Nikon Diaphot epifluorescence microscope with 20× Fluor objective (Nikon), Hamamatsu C2400 silicon-intensified target camera, and a Sony VHS video tape recorder. Wave analysis was done off-line on a MegaVision 1024XM image processor (MegaVision, Santa Barbara, CA) frame by frame from data transferred from tape to a Panasonic TQ-2028F optical disk recorder. In this microscope and image-processing system, 1 pixel = 0.86 μm.

Ca^{2+} kinetics were resolved by monitoring the cells continuously for up to 60 s at 380 nm excitation after first obtaining F_{340}/F_{380}. Based on previous ratiometric calibrations, we established that from a resting $[Ca^{2+}]_i$ level of 30 to 110 nM (68 ± 39 nM, 182 cells), a 25% change in F_{380} corresponds to a change in $[Ca^{2+}]_i$ of 126 ± 15 nM (Wang and Thompson, 1994).

Fura-2 dextran, 70,000 MW, was dissolved at a concentration of 1 mM in saline containing (mM) NaCl 5, KCl 140, $MgCl_2$ 2, HEPES 10, pH 7.2, at 20°C and injected using an Eppendorf microinjector. Assuming that injection volumes are no more than 5% of the cell volume, the concentration of dextran in cells is 50 μM or less.

Wave analysis

Calcium waves were usually evoked by bath application of 1 mM carbachol. In cell passages with low responsiveness to carbachol, 10 or 20 μM histamine was used instead. Calcium waves were identified by eye by reviewing data played back at 1–5 times normal speed. For quantitative analysis, a line segment passing through the cell in the direction of wave propagation was selected. Fluorescence was averaged over one to four

pixels on both sides of the line segment (Fig. 1 *B*, black bar), at a rate of 30 frames/s. Baseline fluorescence, F_0, was defined as the background-subtracted fluorescence along the segment averaged over 10 frames immediately preceding agonist exposure. The fluorescence signal was converted to units of $\% \Delta F/F_0$. For display, red, green, and blue pseudocolor mapping tables were based on CIF standard color-mixture curves for pure spectral color appearance (Inoué, 1986, p. 87) and were defined so that apparent pseudocolor wavelength was linear with ΔF. Normalized lines of ΔF were stacked to generate images in which the abscissa represents time and the ordinate represents location along the scanned line segment. These images were filtered to display a range of ΔF between 40 and 60% of the peak ΔF of the wave, yielding a graph of wave position against time. The speed of the wave was measured by monitoring two points in the cell Δx apart, measuring the lag in time, Δt, for the wave to cross the 50% peak ΔF points in the two regions, and calculating the speed $v = \Delta x/\Delta t$ (Fig. 1 *C*). In the example shown, the ends of the wave front were chosen for monitoring. This gave results that were in agreement with taking the slope of the wave front position graph. After buffer loading, waves were only accepted for analysis if the wave could still be seen and was unbroken in profile. For accurate determination of wave speed it was necessary for a wave to traverse at least 10 μm.

Estimation of effective buffering by AM-loaded calcium chelators

A functional measure of the degree of calcium-buffering ability of a cell is the parameter κ, the amount of Ca^{2+} bound per unit change in free cytoplasmic Ca^{2+}. This parameter is the sum of the endogenous Ca^{2+} buffering and the buffering by fura-2 introduced by the initial loading procedure (Tank et al., 1991; Neher and Augustine, 1992). As free Ca^{2+} increases buffers may saturate and κ may decrease.

If exogenous buffer is added to cytoplasm, the buffer strength κ will be increased by an amount $\Delta\kappa$ that depends on the amount and physical properties of the exogenous buffer. For a Ca^{2+} buffer B with known affinity K_D for Ca^{2+}, the concentration of bound B is a simple function of

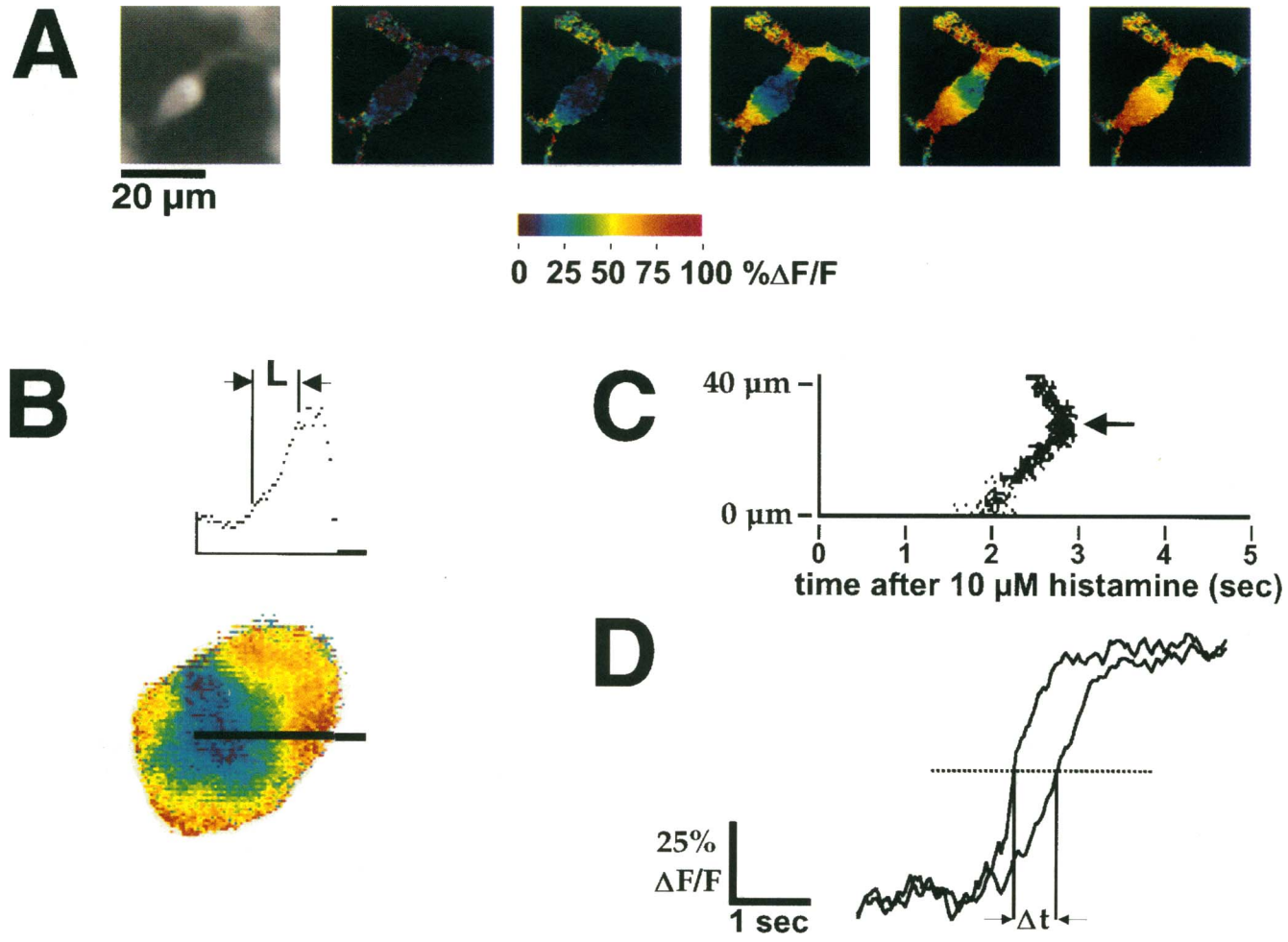

FIGURE 1 Calcium release waves in N1E-115 cells. (*A*) An example of spatially complex Ca^{2+} release. The left-hand panel shows a gray-scale image of fluorescence at 380 nm excitation. In color panels, fura-2 fluorescence is shown as $\Delta F/F_0$ at 380 nm excitation (see Materials and Methods). Images (10-frame averages) were taken at 0.67-s intervals starting 1 s after applying 1 mM carbachol. The Ca^{2+} release starting in the lower left region of the cell was accepted for wave analysis; the Ca^{2+} release starting in the upper right was not. (*B*) Wave front length determination. The image shows $\Delta F/F_0$ 3.4 s after applying 10 μM histamine to a cell injected with fura-2 dextran, 70,000 MW. ΔF was averaged in a 9 pixel-wide region of interest indicated by the black bar superimposed on the image of the cell. The length of the wave front is defined as the distance between 10% and 90% maximum $\Delta F/F_0$ (*vertical lines*). In this example $L = 14$ μm. (*C*) Uniformity of wave speed. Points along the bar in *B* with $30\% < \Delta F/F_0 < 50\%$ (*yellow and yellow-green*) are plotted against time. The $x = 0$ μm point corresponds to the right edge of the cell. The speed of the wave remains constant until it is annihilated in a collision with another wave (*arrow*). (*D*) Wave speed determination. The graph shows fluorescence at two points $\Delta x = 13$ μm apart. The wave front location, defined as the point where ΔF is 50% of maximum, arrived $\Delta t = 0.57$ s later at the second point. The speed of this wave was $v = \Delta x/\Delta t = 23$ μm/s.

$[Ca^{2+}]_i$: $[B]_{bound} = [B]_{total}\,[Ca^{2+}]_i/([Ca^{2+}]_i + K_D)$. The buffer capacity of B is then

$$\Delta\kappa = \frac{d[B]_{bound}}{d[Ca^{2+}]_i} = \frac{[B]_{total}K_D}{([Ca^{2+}]_i + K_D)^2}, \quad (1)$$

where $[B]_{total}$ is the total amount of added buffer. For this relation to hold, it is necessary for $[Ca^{2+}]_i$ to be the same before and after loading with B. This is the same as Zhou and Neher's expression for κ_B (Zhou and Neher, 1993, eq. 9). This expression for $\Delta\kappa$ reaches a maximum as a function of K_D when $K_D = [Ca]_i$.

According to these definitions of κ and $\Delta\kappa$, a calcium flux J will cause $[Ca^{2+}]_i$ to increase at an initial rate of $d[Ca^{2+}]_i/dt = J/(1 + \kappa)$ and at rate $J/(1 + \kappa + \Delta\kappa)$ after the additional buffer load. The response to a given flux of calcium will therefore be attenuated by a factor $A = (1 + \kappa)/(1 + \kappa + \Delta\kappa)$. Rearranging, this gives $\Delta\kappa = (1/A - 1)(\kappa + 1)$. Substitution of this into the left-hand side of Eq. 1 and solving gives

$$\frac{[B]_{total}}{\kappa + 1} = \frac{(1/A - 1)([Ca^{2+}]_i + K_D)^2}{K_D}. \quad (2)$$

This equation allows the relative total added buffer concentration, $[B]_{total}/(\kappa + 1)$, to be estimated from measurements of the cellular response to a fixed flux of Ca^{2+}.

We used $[B]_{total}/(\kappa + 1)$ as a measure of the relative degree to which various AM-esterified buffers could be loaded into cells. A flux of Ca^{2+} was induced by depolarizing cells with high-potassium saline. Depolarization opens both transient and long-lasting voltage-gated calcium current. At these buffer loads, which are much lower than that required to block calcium-dependent inactivation (Stern, 1992), the fluxes before and after loading will be the same. The calcium influx was taken by measuring steady-state $d[Ca^{2+}]_i/dt$ after 1–5 s of high K stimulation (Fig. 2 *A*). We did not undertake an independent measurement of κ, which has been estimated to be 50–200 in other preparations (Hodgkin and Keynes, 1957; Baker and Crawford, 1972; Neher and Augustine, 1992; Zhou and Neher, 1993; Guerrero et al., 1994; Tse et al., 1994).

RESULTS

The activation of M1 muscarinic receptors or histamine receptors by agonist elicits calcium waves in N1E-115 neuroblastoma cells loaded with fura-2/AM. Calcium waves propagate rapidly to invade all parts of the cell, including the processes, and the peak change in $[Ca^{2+}]_i$ occurs as much as 2 s apart in distant regions of the same cell. The Ca^{2+} rise begins with a delay of 1 to 20 s after agonist application, and this delay can be explained by a model in which IP_3 must accumulate to a threshold concentration before activating Ca^{2+} release (Wang et al., 1995). Calcium waves were observed in 11 ± 6% SD of the cells (71 of 723 cells in 19 experiments). Oscillations in $[Ca^{2+}]_i$ were rare, and in most cases only a single calcium wave was observed to cross-the cell. In two experiments on cells microinjected with fura-2 dextran, 8 of 16 cells generated calcium waves. This shows that wave propagation does not require the presence of a mobile Ca^{2+} indicator.

In many cases, the spread of calcium release could be observed as a well-defined wave front crossing the cell. An example is shown in Fig. 1 *A*. The cell was stimulated by rapid bath application of carbachol (1 mM) which elicited a calcium wave starting at the lower left region of the cell body and spreading to the upper right. This calcium wave

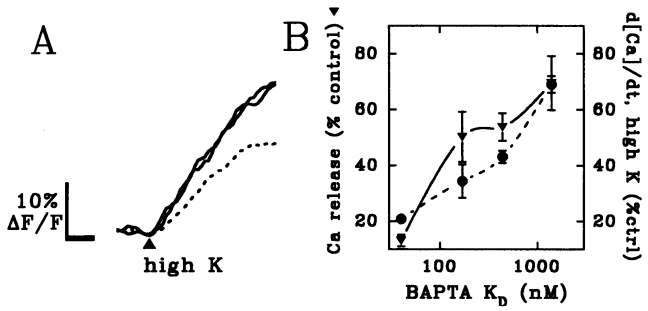

FIGURE 2 Changes in $[Ca^{2+}]_i$ buffering due to AM ester loading. (*A*) The initial rate of rise in $[Ca^{2+}]_i$ was measured in response to depolarization by high K. After returning to normal saline and after three intervening agonist applications, a second challenge with high K 60 min later gave the same rate of rise in $[Ca]_i$ (*solid traces*). After additional loading with 2 μM fura-2/AM for 30 min the slope of the response was markedly lower (*dashed trace*). This change in slope was used to calculate the relative increase in Ca^{2+} buffering contributed by the second fura-2/AM load (see Materials and Methods). (*B*) Attenuation factor, *A*, of whole-cell elevations in $[Ca^{2+}]_i$ as a function of buffer affinity (K_D). *A* was measured for high K-induced Ca^{2+} entry (*circles, dashed curve*) and agonist-induced Ca^{2+} release (*triangles, solid curve*). In both cases, attenuation of the response increase with Ca^{2+} affinity of the buffer.

was accepted for analysis (see Materials and Methods). In contrast, the pattern of calcium release in the upper right region of the cell was not unidirectional and did not propagate for a sufficient distance for wave speed to be measured, and so was rejected from the analysis. When two points in the direction of wave propagation were monitored, the peak change in fluorescence attained at the two points was the same (Fig. 1 *D*), showing that the Ca^{2+} wave does not diminish in amplitude as it travels.

A wave was defined as passing a point when ΔF reached 50% of its maximum change at that point. Wave speed was determined by measuring the time difference as the wave front passed two points in the cell (see Fig. 1 *D* and Materials and Methods). A plot of wave front position against time shows that the front can travel for many microns at roughly constant speed (Fig. 1 *C*). In cells that were accepted for analysis, the wave front traveled in an uninterrupted fashion for at least 10 μm. In some cases the wave disappeared after colliding with another wave (Fig. 1 *C*, arrow). This is consistent with a reaction-diffusion process in which Ca^{2+} release is inactivated or depleted by the passing of a wave (Lechleiter et al., 1991).

The length of the wave front *L* was measured by taking an image of the propagating wave and measuring the distance, in the direction of propagation, between the points where the fluorescence signal equals 10% and 90% of the maximum $\Delta F/F$ (Fig. 1 *B*). Wave front length was measured only when the entire front was visible at one time and noise in the signal was low enough for the 10% and 90% crossing points to be located by eye. Wave speeds ranged from 12 to 146 μm/s (43 ± 28 μm/s, SD, 22 cells), and calcium wave fronts were 3.5 to 22 μm in length (13.3 ± 5.5 μm, SD, 14 cells).

TABLE 1 Efficacy of AM-loading with EGTA and BAPTA-family Ca^{2+} chelators

Chelator/loading conditions	Attenuation factor, A	K_D (nM)	$[B]_{total}/(\kappa + 1)$ (μM)
30 min, 2 μM, 23°C			
EGTA/AM	0.73 ± 0.11	70	0.10
5,5′-dimethyl-BAPTA/AM	0.20 ± 0.04	150	1.29
fura-2/AM	0.35 ± 0.04	170	0.63
BAPTA/AM	0.43 ± 0.02	440	0.78
5,5′-Br_2-BAPTA/AM	0.69 ± 0.03	1580	0.77
30 min, 5 μM, 23°C			
EGTA/AM	0.43 ± 0.03	70	0.37
60 min, 5 μM, 31°C			
EGTA/AM	0.16 ± 0.01	70	1.47

K_D values are for saline of mammalian ionic strength at pH 7.4, 30°C, and are taken or extrapolated from Pethig et al. (1989) and Pozzan and Tsien (1989).

Effects of exogenous buffers on Ca^{2+} signals

Ca^{2+} influx was evoked by rapidly depolarizing cells with a high-potassium saline to activate both transient and long-lasting voltage-dependent Ca^{2+} currents, a procedure that elevates free $[Ca^{2+}]_i$ (Fig. 2 *A*). The steady-state slope of the initial rise in $[Ca^{2+}]_i$ was measured before and after loading cells with additional Ca^{2+} buffers, and changes in this slope were used to infer the amount of added buffer. After measuring the response to high-potassium saline under control conditions, one of four BAPTA-series buffers, with K_D for Ca^{2+} ranging from 70 to 1580 nM, was AM-loaded into cells. After loading, the change in $[Ca^{2+}]_i$ on perfusion with high K saline was measured again, and in each case the rate of rise in $[Ca^{2+}]_i$ was lower after loading with additional exogenous buffer (Fig. 2 *A*, dashed trace). The ratio of the second, lower slope to the first defines an attenuation factor *A*.

A was lowest for BAPTA-series buffers with K_D nearest to the resting $[Ca^{2+}]_i$ (Table 1). The degree of loading could be calculated from *A* given the affinity of the buffer (see Materials and Methods) using values of K_D taken from the literature (Pethig et al., 1989). Under our loading conditions (2–5 μM AM ester, 30 min at 23°C), the BAPTA derivatives 5,5′-Br_2-BAPTA/AM, 5,5′-Me_2-BAPTA/AM, and BAPTA/AM loaded equally well, approximately 1.2 times as well as fura-2/AM (Fig. 2 *B*, circles and broken curve). Loading with these compounds increased the exogenous buffer concentration by a factor $[BAPTA]_{total}/(\kappa + 1) = 0.8 \pm 0.3$ μM. Assuming $\kappa = 100$, this corresponds to 80 ± 30 μM total added chelator. Under the same conditions, EGTA/AM loaded poorly, about 0.2 times as well as fura-2/AM. Buffer loading was increased approximately fourfold when the EGTA/AM concentration was raised to 5–10 μM and cells were incubated for 1 h at 31°C. The latter EGTA/AM loading protocol was used in all of the Ca^{2+} wave experiments to allow comparison with results from BAPTA-family chelators.

Loading cells with exogenous Ca^{2+} buffers also reduced the amplitude of agonist-evoked Ca^{2+} release, and

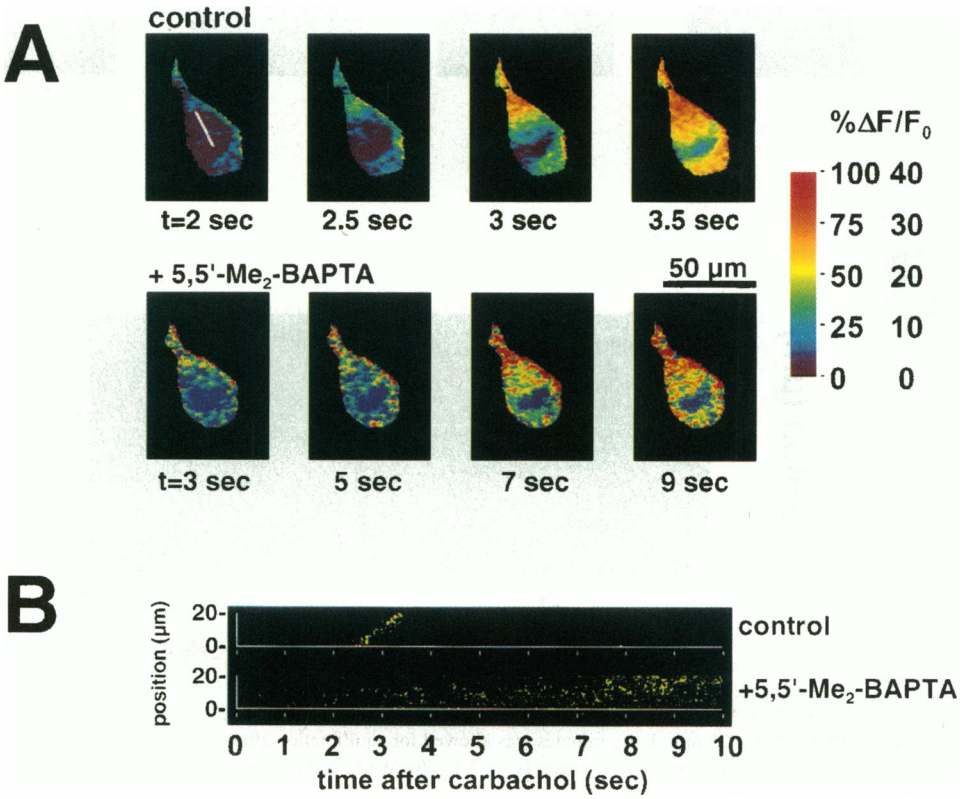

FIGURE 3 5,5′-dimethyl-BAPTA/AM loading slows calcium waves. (*A*) Images (six-frame averages) of a Ca^{2+} wave in response to 1 mM carbachol in control conditions (*upper row of images;* range of ΔF is 0–100%). After loading with 2 μM 5,5′-dimethyl-BAPTA/AM for 30 min and waiting 45 min for equilibration, a second wave was evoked (*lower row;* range of ΔF is 0–40%). (*B*) Progression of the wave was monitored along the white bar shown in the first frame in *A*. Wave speeds are indicated by the slopes of the lines in the twp graphs shown in *B*. The wave speed was 24 μm/s in the control and 4 μm/s after 5,5′-dimethyl-BAPTA/AM loading.

this effect was more pronounced for buffers with K_D near resting $[Ca^{2+}]_i$ (Fig. 2 *B*, triangles). Added buffer attenuated the Ca^{2+} increase in response to agonist to the same extent that it attenuated the Ca^{2+} increases due to depolarization with high-potassium saline. This is consistent with the idea that the total amount of releasable Ca^{2+} is not changed when additional Ca^{2+} buffer is introduced into the cell, but that Ca^{2+} entering the cytosol is chelated to a greater extent.

Testing for Ca^{2+} feedback with buffers: effects on wave profile and speed

We tested the hypothesis that positive feedback by Ca^{2+} represents a rate-limiting step in the propagation of Ca^{2+} waves, reasoning that if calcium acts in positive feedback, then the addition of an exogenous calcium buffer should slow the wave. Calcium waves were measured before and after incubating cells for 30 min in a loading solution containing a high-affinity BAPTA-like Ca^{2+} buffer (2 μM 5,5′-dimethyl-BAPTA/AM; K_D = 150 nM). The calcium wave in Fig. 3 *A* was slowed by this treatment. This is shown more clearly in the series of stacked wave front profiles (Fig. 3 *B*), in which points of equal ΔF are shown as a diagonal band of a single color. The slopes of the bands show a slowing of the wave from 24 μm/s to 4 μm/s. Wave speed decreased in three of four cells (average change in speed in paired comparisons, $-32 \pm 18\%$, mean $\pm$ SEM). The same buffer load also increased the rise time of Ca^{2+} release, from 1.4 ± 0.1 s to 7.0 ± 1.4 s (nine cells in three experiments; Wang et al., 1995), which provides another indication of Ca^{2+} feedback during release.

Is the calcium-dependent regenerative step in wave propagation global or local in nature? If the feedback step is

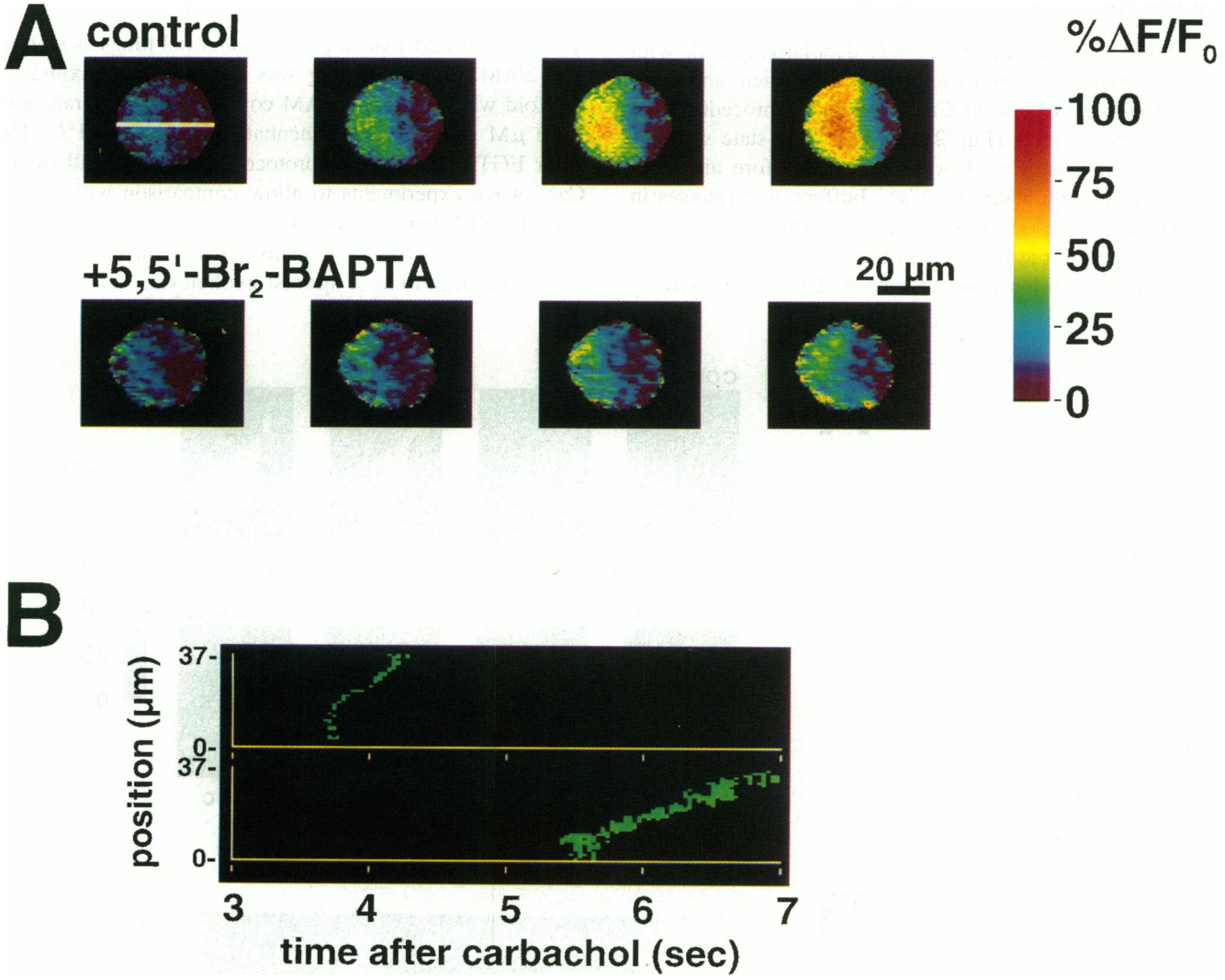

FIGURE 4 5,5′-Br_2-BAPTA/AM loading slows calcium waves. (*A*) Calcium waves in response to 1 mM carbachol before and after loading with 5 μM 5,5′-Br_2-BAPTA/AM for 25 min. Forty minutes was allowed for equilibration after rinsing the chamber with saline. Each image represents the average of four frames, and the interval between images is 0.13 s. (*B*) Wave front profiles. The wave speed was 29 μm/s in the control and 20 μm/s after 5,5′-Br_2-BAPTA/AM loading.

global, then BAPTA and EGTA will slow waves in accordance with their ability to buffer whole-cell Ca^{2+} levels. On the other hand, if the feedback step is local, then exogenous buffers will slow waves in accordance with their ability to capture Ca^{2+} ions emanating from a pore. In this case, BAPTA-series compounds such as 5,5′-dimethyl-BAPTA or fura-2, which bind Ca^{2+} rapidly (10^8 M^{-1} s^{-1}) at a rate that is limited by diffusion (Kao and Tsien, 1988; Baylor and Hollingworth, 1988), will be much more effective in slowing waves than equal amounts of EGTA, which has an on-rate of 10^6 M^{-1} s^{-1} (Tsien, 1980; Neher, 1986).

We found that calcium waves were not slowed by EGTA/AM (K_D = 70 nM). In the cell shown in Fig. 5 the wave speed was 30 μm/s under control conditions and 25 μm/s after EGTA/AM loading. The average speed of waves before EGTA/AM loading was 44.1 ± 6.3 μm/s, and 41.0 ± 6.9 μm/s after (SEM; six cells). The average change in wave speed in paired comparisons was +3.5 ± 11.9%. Because the principal difference between EGTA/AM and BAPTA-family buffers is that EGTA has a 100 times slower on-rate for Ca^{2+} binding, we conclude that the feedback role of Ca^{2+} in wave propagation is primarily a local one.

Ca^{2+} buffers may affect wave propagation in other ways. In addition to interrupting local feedback by released Ca^{2+}, added buffer may also influence the Ca^{2+} release mechanism by decreasing the resting Ca^{2+} level in the cell. It has been shown that resting $[Ca^{2+}]_i$ influences Ca^{2+} wave speed (Girard and Clapham, 1992). In the present experiments, resting $[Ca^{2+}]_i$ was not changed significantly by loading with BAPTA-family AM esters (Table 2). This shows that changes in resting $[Ca^{2+}]_i$ are not responsible for the slowing of Ca^{2+} waves that we observe.

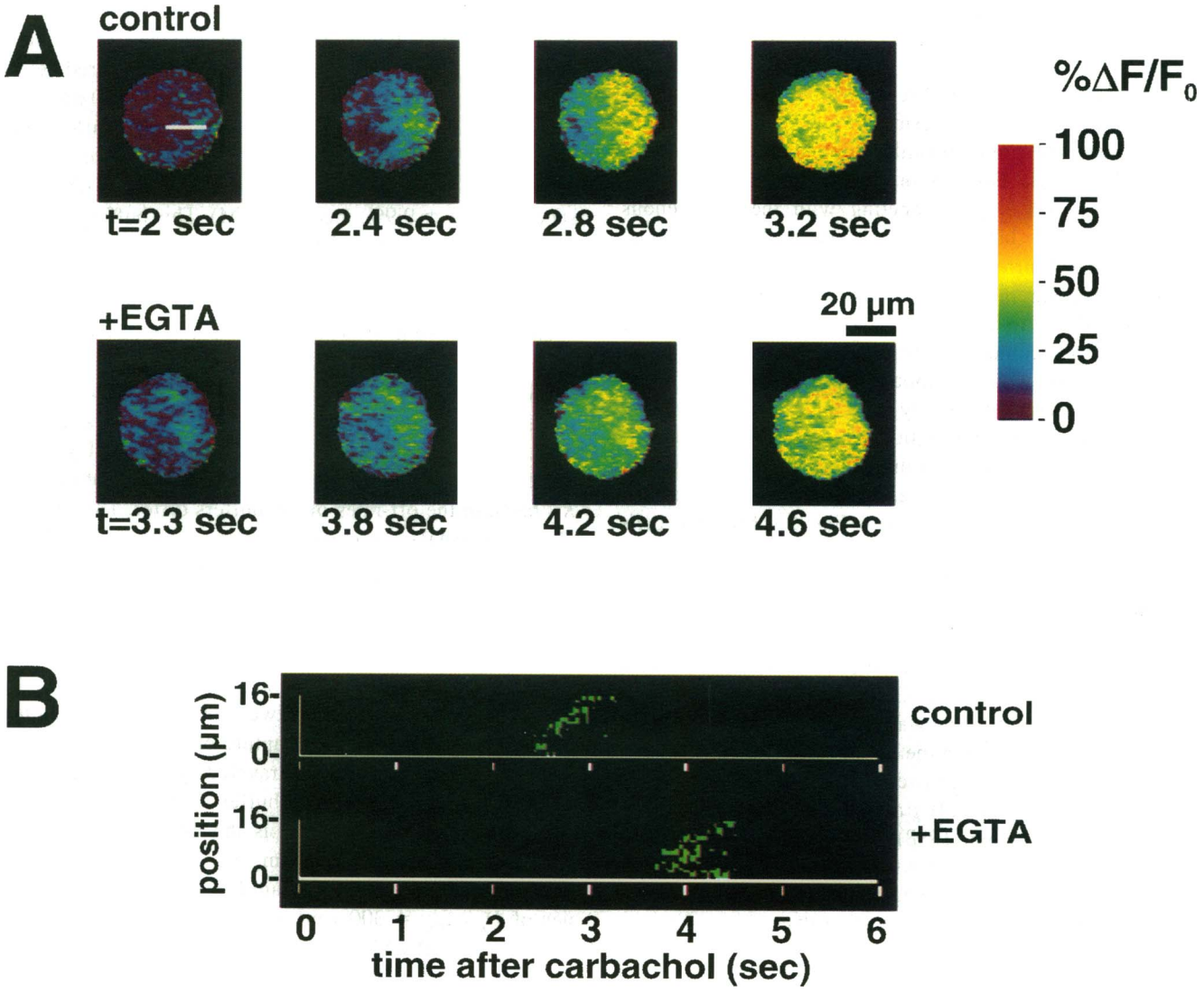

FIGURE 5 EGTA/AM loading does not slow calcium waves. (*A*) Calcium waves in response to 1 mM carbachol before (six-frame averages) and after loading with 5 μM EGTA/AM for 60 min at 31°C and after a 55-min equilibration period. The white line in the first panel shows the region of interest in the direction of wave propagation. (*B*) Wave front profiles before buffer loading (*upper trace*) and after loading (*lower trace*). The wave speed was 30 μm/s in the control and 25 μm/s after EGTA/AM loading.

TABLE 2 Effects of buffer loading on Ca^{2+} wave parameters in N1E-115 cells

	BAPTA-family buffers (16 cells)		EGTA (6 cells)	
	Control	After loading	Control	After loading
Resting $[Ca^{2+}]_i$	98 ± 21 nM	118 ± 20 nM	N/D	N/D
$\Delta F/F$ at 15 s	45.4 ± 3.3%	35.2 ± 4.3%*	55.1 ± 3.6%	40.8 ± 3.7%‡
Wave speed (μm/s)	42.5 ± 8.0	26.5 ± 5.2*	44.1 ± 6.3	41.0 ± 6.9
Change in wave speed (%)		−26.9 ± 9.3%‡		+3.5 ± 11.9%

*Significantly less than control by Student's one-tailed t-test, $0.01 < p \leq 0.05$.
‡Significant less than control by Student's one-tailed t-test, $0.001 < p \leq 0.01$.

As a control for the introduction of AM ester hydrolysis products, cells were loaded with the nonbuffering compound half-BAPTA/AM (10 μM, 30–50 min). This compound, which is smaller and more hydrophobic than the calcium buffers, is expected to load at least as well as the BAPTA/AM compounds. Half-BAPTA/AM had no effect on wave speed or amplitude, showing that AM ester loading alone could not account for changes in wave speed.

Chelators such as BAPTA and EGTA also alter the diffusion of Ca^{2+} in cytoplasm. Because endogenous, cellular buffers are predominantly immobile, one effect of adding the mobile BAPTA or EGTA would be to speed movement of Ca^{2+} by competing with the endogenous buffers for Ca^{2+} binding. For example, the wave front appeared to be blurred by EGTA/AM loading (Fig. 5). This could be a measurement artifact associated with the reduced signal-to-noise ratio of the signal. Alternatively, blurring of the wave front could be a result of facilitated diffusion, because EGTA would compete for released Ca^{2+} that would otherwise be slowed by immobile buffers.

We considered the possibility that such a facilitated diffusion effect is necessary for the generation of Ca^{2+} waves and that waves are, therefore, an artifact caused by the presence of mobile indicator dyes. Fig. 6 shows two cells initially injected with the poorly mobile indicator fura-2 dextran (70,000 MW). Both cells exhibited spatially complex patterns of calcium release when stimulated with carbachol. We conclude that these cells produce Ca^{2+} waves without the need for added mobile dye. These cells were next loaded with 6 μM fura-2/AM for 40 min. After this treatment the calcium wave was slowed in the top cell from 10 μm/s to 6 μm/s, and in the bottom cell from 13 μm/s to 9 μm/s. Because the estimated diffusion constant of this fura-2 dextran is about 50 $\mu m^2/s$ (Callaghan and Pinder, 1983; Pusch and Neher, 1988), as compared to 500 $\mu m^2/s$ for fura-2 (Timmerman and Ashley, 1986), the wave slowing caused by introducing exogenous buffer is independent of the mobility of the initial reporting dye.

Dependence on K_D

We sought to determine whether the ability of BAPTA compounds to slow waves is related to their dissociation constant for Ca^{2+} binding. Four BAPTA-series buffers, with K_D for Ca^{2+} ranging from 70 to 1580 nM, were AM-loaded into cells. Calcium waves were elicited by bath application of carbachol (1 mM), and wave speeds were measured before and after loading with additional buffer.

Fig. 4 *A* shows the results of an experiment using 5,5′-Br_2-BAPTA/AM (K_D = 1580 nM), a compound of approximately ten times lower affinity for Ca^{2+} than 5,5′-dimethyl-BAPTA. Once again, Ca^{2+} waves were measured before and after incubating cells with 5 μM buffer for 30 min. The calcium wave was slowed from 29 μm/s to 20 μm/s by this treatment (Fig. 4 *B*). Wave speed decreased in four of five cells loaded with 5,5′-Br_2-BAPTA/AM (average change in speed, −13.3 ± 9.9%, mean ± SEM). This buffer load also increased the rise time of Ca^{2+} release from 2.0 ± 0.2 s to 4.1 ± 0.6 s (14 cells in five experiments).

All of the BAPTA compounds were approximately equally effective in slowing the propagation of Ca^{2+} waves (Fig. 7). The average wave speed was 42.5 ± 8.0 μm/s (SEM, 16 cells) before buffer loading and 26.5 ± 5.2 μm/s after loading, corresponding to an average change in wave speed of −26.9 ± 9.3%. All of the BAPTA-family buffers have similar on-rates for Ca^{2+} binding but different K_D because the off-rates of the buffers differ. The fact that all of the BAPTA compounds were effective in slowing waves shows that this effect is independent of the K_D or off-rate but depends critically on rapid Ca^{2+} binding.

This series of experiments shows that the critical buffer parameter in slowing wave propagation is its on-rate for Ca^{2+}. In combination with the buffer concentration, the on-rate determines the time between the release of a calcium ion into the cytosol and the capture of that ion by a buffer molecule. The mean distance traveled by a free calcium ion before binding to exogenous buffer is $d = (6\ D_{Ca,\ free}/k_+[BAPTA])^{1/2}$, where $D_{Ca,\ free}$ is the diffusion constant of unbound calcium in cytoplasm and k_+ is the on-rate for calcium binding by BAPTA family buffers. Assuming values of $D_{Ca,\ free}$ = 300 $\mu m^2\ s^{-1}$, $k_+ = 10^8\ M^{-1}\ s^{-1}$, and [BAPTA] = 80 μM, then d = 0.5 μm. In comparison, for the endogenous buffer, d = 0.4–1.3 μm ($k_+ = 10^7$-$10^8\ M^{-1}\ s^{-1}$, 100 μM); and for a comparable load of EGTA, d = 5 μm ($k_+ = 10^6\ M^{-1}\ s^{-1}$, 100 μM). BAPTA therefore is comparable with endogenous buffer in capturing calcium ions emerging from a pore, but EGTA is not. The average

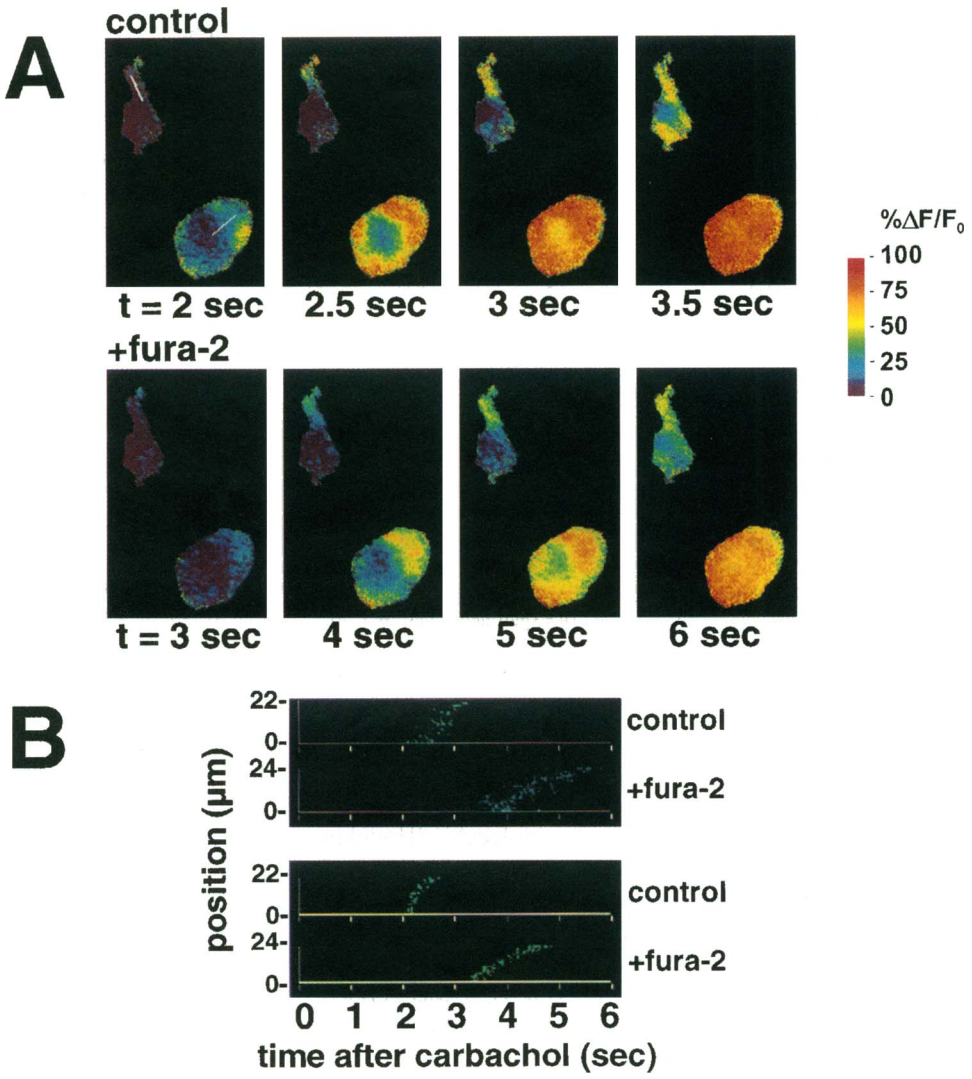

FIGURE 6 Effect of fura-2/AM loading on calcium waves in cells injected with fura-2 dextran, 70,000 MW. (*A*) Calcium waves in response to 10 μM histamine (six-frame averages) measured in two cells before and after loading with 6 μM fura-2/AM for 40 min. The regions of interest are shown by the white lines in the first frame. (*B*) Wave front profiles. In the top cell, the wave speed was 10 μm/s in the control and 6 μm/s after fura-2/AM loading. In the bottom cell, the wave speed was 13 μm/s in the control and 9 μm/s after fura-2/AM loading.

distance of Ca^{2+} action in wave propagation is, therefore, less than 1 μm.

Quantitative analysis of wave fronts

In the theory of reaction-diffusion systems, the free diffusion constant of the feedback messenger is thought to constrain the length, L, and speed, v, of an advancing wave front to obey the relation $D_{free} = L \cdot v + C$ (Luther, 1906; Jaffe, 1991; Sneyd and Kalachev, 1994), where C is a positive correction term that depends on the specific excitatory mechanism and buffer parameters, so that $D_{free} > L \cdot v$. We explored this relationship using values of L and v determined from Ca^{2+} wave fronts.

In cells loaded with fura-2/AM, the product $L \cdot v$ varied from 140 to 700 $\mu m^2/s$ (399 $\pm$ 193 $\mu m^2/s$, SD, 13 cells). Measurements of $L \cdot v$ in cells injected with fura-2 dextran (70,000 MW) gave similar values (234 and 554 $\mu m^2/s$, 2 cells), showing that $L \cdot v$ was not dependent on the mobility of the indicator dye. These values are in the same range as values for other Ca^{2+} wave systems (Jaffe, 1991; Meyer, 1991). The value of $L \cdot v$ is plotted in Fig. 8 *A* along with the diffusion constants for IP_3 and Ca^{2+}. The product $L \cdot v$ is near the diffusion constant of IP_3 (280 $\mu m^2/s$) (Allbritton et al., 1992) and the diffusion constant of unbuffered calcium in aqueous solution (200–600 $\mu m^2/s$) (Robinson and Stokes, 1955; Hodgkin and Keynes, 1957), but it is much greater than the apparent diffusion constant for buffered calcium in cytoplasm (10–20 $\mu m^2/s$) (Baker and Crawford, 1972).

The results of buffer-loading experiments employing BAPTA-family buffers and EGTA demonstrate that local Ca^{2+} diffusion is an important rate-limiting step in the propagation of Ca^{2+} waves. Therefore, we interpret this wave front analysis in terms of Ca^{2+} diffusion rather than IP_3 diffusion and conclude that $L \cdot v$ gives the apparent diffusion constant (D_{app}) of calcium acting in feedback. Because the product $L \cdot v$ takes a range of values similar to $D_{Ca,\ free}$ but much greater than $D_{Ca,\ buffered}$, calcium ions must close the feedback loop before they are captured by buffer and, therefore, before diffusion is drastically slowed

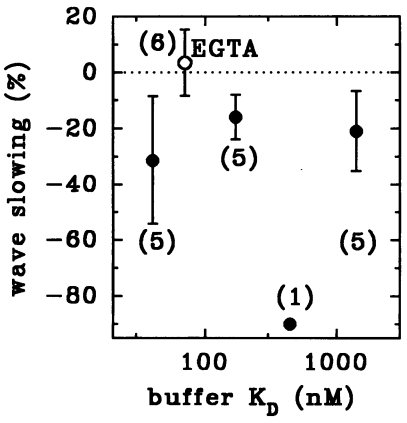

FIGURE 7 The effect of calcium buffers on wave parameters. Calcium waves were measured before and after loading with AM esters of various Ca^{2+} buffers. The change in Ca^{2+} wave speed, expressed as a percentage, is shown as a function of buffer K_D for the BAPTA-series buffers 5,5′-dimethyl-BAPTA/AM, fura-2/AM, BAPTA/AM, and 5,5′-Br_2-BAPTA/AM (*filled symbols*) and for EGTA/AM (*open symbol*). The numbers in parentheses indicate the number of experiments analyzed. All of the BAPTA buffers slowed wave speed by approximately 30%, except for BAPTA itself (one cell). The slow buffer EGTA had no effect on wave speed.

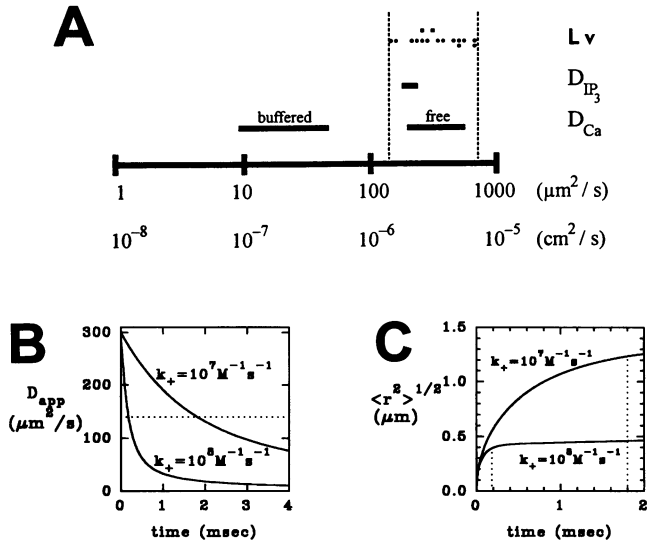

FIGURE 8 The diffusion constant of the feedback messenger predicted from wave front analysis. (*A*) Comparison of the length-speed product, $L \cdot v$, with measured cytoplasmic diffusion constants. Wave fronts were measured in cells loaded with fura-2/AM (●) or injected with fura-2 dextran, 70,000 MW (■). Bars indicate published diffusion constants for free Ca^{2+} (Robinson and Stokes, 1955; Hodgkin and Keynes, 1957; Allbritton et al., 1992), buffered Ca^{2+} in cytoplasm (Baker and Crawford, 1972; Allbritton et al., 1992), and IP_3 in cytoplasm (Allbritton et al., 1992). (*B*) Apparent diffusion constant of Ca^{2+} as a function of time. This was calculated assuming $D_{Ca,\ bound} = 7\ \mu m^2/s$ and $D_{Ca,\ free} = 300\ \mu m^2/s$ and for two values of Ca^{2+} on-rate of the buffer. (*C*) Root-mean squared displacement of Ca^{2+} as a function of time. Conversion to distance from the curves in *B* was done by calculating $\langle r^2 \rangle = 6 \int D_{app}(t')dt'$ (see Materials and Methods). The dotted vertical lines indicate times at which D_{app} reaches 140 $\mu m^2/s$, the smallest value experimentally measured.

by binding with poorly mobile buffer molecules (Hodgkin and Keynes, 1957).

How far from an open channel can Ca^{2+} diffuse freely? We calculated the apparent diffusion constant for Ca^{2+}, D_{app}, for the physiological case of ions emerging from a channel into heavily buffered cytoplasm. D_{app} was defined in analogy with the conventional diffusion constant: $D_{app} \equiv \langle r^2 \rangle / 6t$. The calculation assumed that there was 100 μM cytoplasmic buffer with Ca^{2+} buffering capacity $\kappa = 100$ (see Appendix and Electronic Supplement). The on-rate for Ca^{2+} binding, k_+, was assumed to be either 10^8 or $10^7\ M^{-1}\ s^{-1}$. The results are shown in Fig. 8 *B*, where the dotted line at $D_{app} = 140\ \mu m^2/s$ indicates the lowest value of $L \cdot v$ observed in experiments. D_{app} drops to this level after 0.2 ms when $k_+ = 10^8\ M^{-1}\ s^{-1}$ and after 1.9 ms when $k_+ = 10^7\ M^{-1}\ s^{-1}$ (Fig. 8 *B*). The spatial range of calcium feedback action can be estimated by calculating the mean-squared displacement of all the calcium ions during this time (Fig. 8 *C*). At the time that D_{app} drops to 140 $\mu m^2/s$ (dotted lines, Fig. 8 *C*), the root-mean-squared displacement of calcium is 0.4 μm for $k_+ = 10^8\ M^{-1}\ s^{-1}$ and 1.2 μm for $k_+ = 10^7\ M^{-1}\ s^{-1}$.

DISCUSSION

Calcium waves in N1E-115 cells are regenerative and require fast, local diffusion of Ca^{2+} for propagation to occur. This is demonstrated by the observation that progression of the wave is slowed by the addition of BAPTA Ca^{2+} buffers that have fast on-rates, but not by EGTA, which has a much slower on-rate. We conclude that BAPTA compounds reduce wave speed by interrupting a rapid Ca^{2+} feedback step in the propagation mechanism. Furthermore, we used the length-speed product of advancing wave fronts to show that Ca^{2+} acting in feedback diffuses at nearly the rate of free diffusion during this step. Because cytoplasm contains a fast and immobile endogenous buffer, this rate of diffusion can only occur within 1 micron of the channel and for less than 1 ms after ions emerge from an open channel.

It has been shown that photolytically induced elevation of IP_3 elicits Ca^{2+} waves in *Xenopus* oocytes, demonstrating that steps downstream of IP_3 production are sufficient for wave propagation to occur (Lechleiter and Clapham, 1992). Our experiments show that local Ca^{2+} diffusion is a necessary step in an agonist-evoked Ca^{2+} wave. Together, these lines of evidence confirm a proposed mechanism of wave propagation that relies on calcium-induced calcium release (Jaffe, 1983; Backx et al., 1989), specifically by Ca^{2+} feedback on IP_3 receptors (Lechleiter et al., 1991). We showed that regenerative Ca^{2+} release follows a period in which IP_3 builds to a threshold (Wang et al., 1995) and now present a full model of the steps that produce a calcium wave.

Model for calcium wave propagation

Our data support a propagation mechanism in which receptor-activated phospholipase C generates IP_3 until threshold levels of IP_3 are reached (Fig. 9). At low $[Ca^{2+}]_i$, IP_3-bound receptors are unlikely to open. When spontaneous openings do occur, the nearest-neighbor IP_3-bound receptor is on average too far away for the released Ca^{2+} to diffuse to it. However, when IP_3 reaches threshold, bound receptors are spaced closely enough that calcium release beginning at one receptor can bring neighboring IP_3 receptors to threshold for release. The resulting calcium release closes the feedback loop, allowing further propagation of the calcium wave. This feedback takes place between IP_3 receptors that are less than 1 μm apart.

The distance between IP_3 receptors can be estimated from published binding data. Information for N1E-115 cells is not available, but sufficient information can be found for another preparation that exhibits regenerative Ca^{2+} release: guinea pig hepatocytes, which contain approximately 200 fmol IP_3 binding sites/mg protein (Spät et al., 1986). Based on an estimate of 2.2 μl intracellular water/mg protein (De Witt and Putney, 1984), a conversion to cell volume gives 5.5 IP_3 binding sites/μm^3 of hepatocyte. Using the nearest-neighbor formula for randomly distributed particles at density n, $d = 0.55\ n^{-1/3}$ (Chandrasekhar, 1943), this gives an average distance between IP_3 receptors of 0.3 μm if the IP_3 receptor has one binding site for IP_3, and 0.5 μm if it has four. IP_3 receptors are not randomly distributed but rather decorate the surface of the ER, and so on average they may be closer together than indicated by this calculation. These numbers are consistent with our proposed wave propagation mechanism if feedback occurs between a channel and its nearest neighbors.

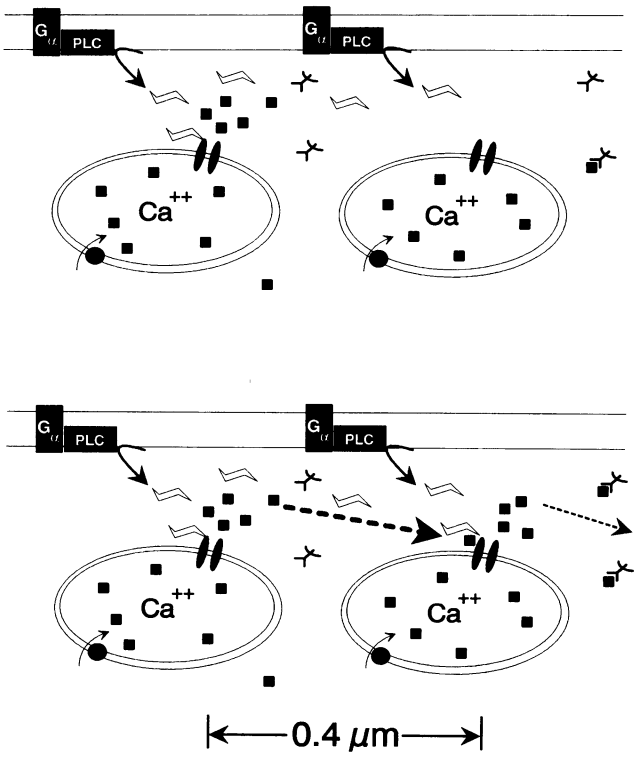

FIGURE 9 Proposed mechanism of calcium wave propagation in N1E-115 cells. After application of agonist, activation of PLC causes accumulation of IP_3 to threshold levels for Ca^{2+} release (*top*). Release then propagates across the cell, with local Ca^{2+} diffusion as the rate-limiting feedback step (*bottom*). This diffusion is local, and on average, cytoplasmic Ca^{2+} buffers (*anchor-shaped symbols*) are unable to slow the diffusion before the positive feedback loop is closed.

Comparison of $L \cdot v$ with the time-dependent D_{app} suggests that Ca^{2+} has its feedback effect within no more than 2 ms of entering cytoplasm. This implies that released Ca^{2+} binds to the IP_3 receptor within that time. The speed of this step is not well measured, but the most time-resolved studies so far indicate that the combined steps of binding to Ca^{2+} and the resulting activation of Ca^{2+} release can take place in several tens of milliseconds (Finch et al., 1991; Iino and Endo, 1992).

A potential complicating factor in interpreting the effect of added BAPTA on calcium waves is the observation that BAPTA may also block the IP_3 receptor directly. BAPTA has been observed to bind to cerebellar IP_3 receptors and inhibit their activity at low concentrations of IP_3 (Richardson and Taylor, 1993), but not at saturating levels of IP_3 (Finch and Goldin, 1994). Given that the observed IC_{50} of BAPTA against IP_3-induced Ca^{2+} release is 1.8 mM (Richardson and Taylor, 1993), our estimated BAPTA load of 80 μM would inhibit up to 4% of IP_3-mediated Ca^{2+} release. This is much less than the attenuation of the Ca^{2+} signal that was actually observed (Fig. 2), and therefore we conclude that BAPTA attenuates elevations of cytoplasmic Ca^{2+} primarily by buffering Ca^{2+}.

Measurement of IP_3 receptor density in N1E-115 cells is necessary to test our model of wave propagation. We predict that N1E-115 cells will have at least as high a concentration of IP_3 receptors as hepatocytes. This suggests that it may be possible to alter wave parameters by partially blocking IP_3 receptor function, which would increase the average distance that Ca^{2+} has to travel to cause feedback.

Interpreting wave front parameters in a buffered cytoplasm

Wave parameters have been used before in attempts to infer the mobility of the factor that limits wave propagation. Those analyses suggested that the diffusible factor has a diffusion constant greater than 200 $\mu m^2/s$, based on two types of measurements: the relationship between wavefront curvature and speed (Lechleiter et al., 1991), and the length-speed product of wavefronts (Luther, 1906; Jaffe, 1991; Meyer, 1991). In both cases the predicted diffusion constant was found to be near both D_{IP3} and $D_{Ca,free}$, and these measures have been variously interpreted as meaning that the limiting messenger in wave propagation is IP_3 (Allbritton et al., 1992) or Ca^{2+} (Jaffe, 1991; Lechleiter et al., 1991).

In the wavefront curvature analysis (Lechleiter et al., 1991) identification of the feedback messenger was predicated on comparing its diffusion constant with known diffusion constants of IP_3 and Ca^{2+}. This was based on a two-species model of wave propagation (Keener and Tyson, 1986; Tyson and Keener, 1988). The feedback messenger can be potentially identified by its diffusion constant if the species diffuse at unequal rates. However, accurate diffusion constants for IP_3 and Ca^{2+} were unavailable at the time.

An issue overlooked in both kinds of analysis is that the diffusion constant of Ca^{2+} varies with time after it exits the channel and enters the buffered environment of cytoplasm. Because the range of $D_{Ca,app}$ overlaps D_{IP3}, inferences of the diffusion constant of the feedback messenger cannot be used to choose a priori between IP_3 and Ca^{2+}. Our alternative approach to this problem was to study the effects of fast and slow buffers to establish independently that Ca^{2+} diffusion is rate-limiting. $L \cdot v$ and the time dependence of the diffusion "constant" of Ca^{2+} were then used to calculate the range of action of Ca^{2+} feedback.

The theoretical basis for our work depends on several assumptions. The interpretation of $L \cdot v$ as a diffusion constant assumes that 1) $D_{app} > L \cdot v$, and 2) video fluorescence measurements of the fura-2 fluorescence profile give accurate determinations of L and v.

The interpretation of $L \cdot v$ as an apparent diffusion constant is based on theoretical analyses of unbuffered chemical reaction-diffusion systems. The presence of buffers means that only a fraction of the calcium ions entering cytoplasm remain free. Also, the diffusion properties of the ions are altered if the buffers are of different mobility than free Ca^{2+}. Various aspects of buffering have been considered (Sneyd and Kalachev, 1994; Bezprozvanny, 1994; Wagner and Keizer, 1994), but so far the finite binding kinetics of buffers and the microscopic spacing of IP_3 receptors have not been fully taken into account. Microscopic modeling is essential because IP_3 receptor spacing is in a range over which the time dependence of Ca^{2+} diffusion is significant. Our approach here has been to calculate a time-dependent D_{app}. These problems must be addressed by rigorous theoretical work before final judgment of this type of wave front analysis can be made.

The front of increased Ca^{2+} is assumed to represent the front of Ca^{2+} release activity as it crosses the cell. This would not necessarily be the case if fura-2 acted to facilitate the diffusion of Ca^{2+} from its release site and thus flattened the profile of a Ca^{2+} wave compared with the distribution of open channels. Two Ca^{2+} indicators with markedly different mobilities, AM-loaded fura-2 (which yields the free acid, 768 MW), and fura-2 dextran, 70,000 MW, gave the same range of values for $L \cdot v$, suggesting that facilitated diffusion does not distort the wavefront. However, the observation that waves were observed more often in fura-dextran-injected cells (50%) than in AM-loaded cells (11%) suggests that gradients are more difficult to observe with a mobile indicator.

Uncertainties in wave front measurements

Conventional fluorescence microscopy underestimates the true wave speed if the wave travels at a vertical angle to the plane of focus or at a horizontal angle to the direction monitored. Assuming that waves propagating at more than 20° to the plane of focus would travel out of the plane of view or be indistinct, the front speed would be underestimated by no more than $100(1 - \cos 20°) = 6\%$. The front length is also potentially underestimated by the same amount, 6%.

Conversely, the wave front length could be overestimated if advancing wave fronts are out of register with the in-focus wave front. N1E-115 neuroblastoma cells are approximately hemispherical in shape, giving a 20 μm cell thickness for a 40 μm cell. In epifluorescence imaging conditions, fluorescent latex microspheres are nearly undetectable as near as several microns out of the plane of focus (Blumenfeld et al., 1992), and so large defocused contributions to the front signal are unlikely.

The length of the wave front may also be overestimated because of camera lag. At levels of image intensity comparable to fluorescence images, our SIT camera adapts to a shutter opening or closing with a time constant of about 6 frames (0.17 s). If a wave front is traveling rapidly, the image formed by the camera will be a composite of wave fronts, averaged over a window of 0.17 s. A wave traveling at 20 μm/s moves 3.4 μm during this time. If the wave front is 10 μm long, the measured wave front would be 13.4 μm long, a 34% overestimate.

The principal error in measuring wave front parameters is then the lag of the SIT camera, which may cause significant overestimates of wave front length. We therefore took the smallest observed value of $L \cdot v$, 140 $\mu m^2/s$, as D_{app}. In future experiments more accurate values of L and v can be obtained by using a camera with faster response time, such as a cooled CCD camera, or a confocal microscope.

The properties of cytoplasmic Ca^{2+} buffers affect the analysis

The predicted upper distance limit for the feedback action of calcium depends on our theoretical analysis of calcium diffusion from a channel mouth, which assumed that the endogenous buffer is immobile and nonsaturable and has a fast on-rate. The most sensitive parameter in this analysis was the product of on-rate and free buffer concentration, $k_+ [B]_{free}$. A slower on-rate would increase the range of free calcium diffusion, as would the saturation of buffers near the channel mouth. Experimental physiological evidence suggests that the buffer is of lower affinity than 10^6 M^{-1} ($K_D > 1$ μM; Neher and Augustine, 1992). Also, physical chemistry shows that calcium binding to an unbound ligand is diffusion-limited ($>10^8$ M^{-1} s^{-1}) (Seamon and Kretsinger, 1983), although the binding of protons or Mg^{2+} to Ca^{2+} buffers at resting conditions could slow the apparent on-rate. More accurate measurements of endogenous Ca^{2+}

buffer binding kinetics need to be made to improve the estimate of $D_{Ca,app}$.

Possible roles for IP_3 in wave propagation

These experiments show that local Ca^{2+} feedback assists in generating traveling Ca^{2+} waves. However, there remain two possible roles for IP_3. First, local IP_3 production might, in conjunction with Ca^{2+} release, also limit the speed of wave propagation. In this case a wave of generated IP_3 would accompany the Ca^{2+} wave as it crosses the cell.

IP_3 might also contribute to shaping the Ca^{2+} wave without acting as a feedback element. After agonist stimulation, the initial gradient of IP_3 might set the direction or speed of the Ca^{2+} wave. For instance, if IP_3 reaches threshold for release at one point in a cell while nearby areas are not yet at threshold, that point can serve as the locus for initiation of a wave. This phenomenon has been induced in *Xenopus* oocytes, in which IP_3 was photochemically generated in a confined line, and Ca^{2+} release waves were seen propagating from the site of IP_3 production (Lechleiter and Clapham, 1992). Furthermore, we have observed that at low agonist concentration, the delay preceding the Ca^{2+} wave is longer and the wave is slower (not shown). This would be explained if the IP_3 gradient established before Ca^{2+} wave initiation is shallower when the latency is longer.

APPENDIX: CALCULATING THE APPARENT DIFFUSION CONSTANT OF Ca

Calcium diffusion in cytoplasm is slowed by poorly mobile buffers that bind Ca^{2+} (Hodgkin and Keynes, 1957). This can be expressed by defining an apparent diffusion coefficient in analogy to the conventional diffusion constant using $\langle r^2 \rangle$, the mean squared displacement of the total population of Ca^{2+} ions: $D_{app} \equiv \langle r^2 \rangle / 6t$. In the absence of buffering, D_{app} is equal to the free diffusion constant. This quantity was calculated for Ca^{2+} ions entering the cytosol through a channel and coming into binding equilibrium with a buffer of lower diffusion constant than free Ca^{2+}.

We assume that calcium ions start in a free state and equilibrate with a nonsaturating cytoplasmic Ca^{2+} buffer of mobility D_B with binding and unbinding rate constants k_+ and k_-. Under the condition of nonsaturation, the concentration of free buffer is constant everywhere. This assumption means that the forward and backward binding rate constants are independent of position. The buffer system can then be represented by the ordinary differential equation

$$\begin{aligned} df/dt &= -k_+[B]_{free} f + k_-(1 - f) \\ &= -(k_+[B]_{free} + k_-)f + k_-, \end{aligned} \tag{3}$$

where $f(t)$ is the fraction of ions that are free, takes values between 0 and 1, and begins at $f(0) = 1$. This has the solution $f(t) = (e^{-k'} t + \phi)/(1 + \phi)$, where $k' = k(1 + \phi)$, $k = k_+[B]_{free}$ and $\phi = K_D/[B]_{free}$. In the case of a single nonsaturable buffer, ϕ is also the reciprocal of the buffer capacity, κ (Neher and Augustine, 1992). In this solution, $f(t)$ begins at 1 and relaxes toward binding equilibrium, $f_\infty = \phi/(1 + \phi)$, with time constant $1/k'$.

Growth in the mean squared displacement over time can then be calculated given that at time t, fraction $f(t)$ of the ions are diffusing freely at rate D_F, and fraction $1 - f(t)$ are diffusing at rate D_B. This is described by

$$\begin{aligned} d\langle r^2 \rangle_{total}/dt &= 6\, D_F f + 6\, D_B(1 - f) \\ &= 6(D_F - D_B)f + 6\, D_B, \end{aligned} \tag{4}$$

with $\langle r^2 \rangle = 0$ at $t = 0$. Then

$$\langle r^2 \rangle_{total} = 6 \frac{D_B + D_F\phi}{1 + \phi} t + 6 \frac{(D_F - D_B)(1 - e^{-k't})}{k'(1 + \phi)} \tag{5}$$

and

$$\begin{aligned} D_{app,\,total} &= \frac{\langle r^2(t) \rangle_{total}}{6t} \\ &= \frac{D_B + D_F\,\phi}{1 + \phi} + \frac{(D_F - D_B)(1 - e^{-k't})}{k'(1 + \phi)t} \end{aligned} \tag{6}$$

This calculation gives the same result as a full treatment of the partial differential equations describing diffusion from a pore into a nonsaturating buffer (see Electronic Supplement and Wang, 1994). After Ca^{2+} comes into binding equilibrium ($k't \gg 1$), this result is also in agreement with the results of Wagner and Keizer (1994) for very large K_D (nonsaturability) and of Irving et al. (1990).

The character of the time course of D_{app} is strongly sensitive to the on-rate and quantity of free buffer. To cover the likely range of known physiological measurements, D_{app} and $\langle r^2 \rangle$ were calculated as functions of t for $\phi = 0.01$ and $F = 100\ \mu M$, and buffer on-rates of 10^8 or $10^7\ M^{-1}\ s^{-1}$. The mobilities of free and bound calcium were assumed to be 300 and 7 $\mu m^2/s$, respectively, consistent with physiological (Zhou and Neher, 1993; Neher and Augustine, 1992) and biochemical measurements (Hodgkin and Keynes, 1957; Baker and Crawford, 1972; Allbritton et al., 1992).

Other significant assumptions are that the fura-2 indicator and other heterogeneous mobile buffers are ignored, and that buffers do not saturate. However, saturation of endogenous buffer would be potentially significant only in regions where the free Ca^{2+} is on the order of the buffer concentration (Stern, 1992). Endogenous buffers are present at concentrations of at least tens of micromoles per liter, and under physiological conditions, calcium can only approach D_{free} within tens of nanometers of its entry point from a single channel (Smith and Augustine, 1988). We conclude that saturation does not occur in the distance range of 0.1 μm or greater, the range that concerns us here.

We thank the staff of the Hopkins Marine Station for excellent support through the course of this work. R. W. Aldrich, S. E. Fraser, M. A. Harrington, R. S. Lewis, P. Mitra, and S. J. Smith provided helpful discussion and advice. Work supported by NS14519 to S. T. and MH10088 to S. W.

REFERENCES

Allbritton, N. L., T. Meyer, and L. Stryer. 1992. Range of messenger action of calcium ion and inositol 1,4,5-trisphosphate. *Science.* 258: 1812–1815.

Backx, P. H., P. P. de Tombe, J. H. K. Van Deen, B. J. M. Mulder, and H. E. D. J. ter Keurs. 1989. A model of propagating calcium-induced calcium release mediated by calcium diffusion. *J. Gen. Physiol.* 93:963–977.

Baker, P. F., and A. C. Crawford. 1972. Mobility and transport of magnesium in squid giant axons. *J. Physiol.* 227:855–874.

Baylor, S. M., and S. Hollingworth. 1988. Fura-2 calcium transients in frog skeletal muscle fibres. *J. Physiol.* 403:151–192.

Berridge, M. J. 1993. Inositol trisphosphate and calcium signalling. *Nature.* 361:315–325.

Bezprozvanny, I. 1994. Theoretical analysis of calcium wave propagation based on inositol (1,4,5)-trisphosphate ($InsP_3$) receptor functional properties. *Cell Calcium.* 16:151–166.

Bezprozvanny, I., J. Watras, and B. E. Ehrlich. 1991. Bell-shaped calcium-response curves of Ins(1, 4, 5)P_3- and calcium-gated channels from endoplasmic reticulum of cerebellum. *Nature.* 351:751–754.

Blumenfeld, H., L. Zablow, and B. Sabatini. 1992. Evaluation of cellular mechanisms for modulation of calcium transients using a mathematical model of fura-2 Ca^{2+} imaging in *Aplysia* sensory neurons. *Biophys. J.* 63:1146–1164.

Boitano, S., E. R. Dirksen, and M. J. Sanderson. 1992. Intercellular propagation of calcium waves mediated by inositol trisphosphate. *Science.* 258:292–295.

Callaghan, P. T., and D. N. Pinder. 1983. A pulsed field gradient NMR study of self-diffusion in a polydisperse polymer system: dextran in water. *Macromolecules.* 15:968–973.

Chandrasekhar, S. 1943. Stochastic problems in physics and astronomy. *Rev. Mod. Phys.* 15:1–89. (Reprinted in Selected Papers on Noise and Stochastic Processes. N. Wax, editor. Dover, New York, 1954. 337 pp.)

De Witt, L. M., and J. W. Putney, Jr. 1984. α-adrenergic stimulation of potassium efflux in guinea-pig hepatocytes may involve calcium influx and calcium release. *J. Physiol.* 346:395–407.

DeLisle S., and M. J. Welsh. 1992. Inositol trisphosphate is required for the propagation of calcium waves in Xenopus oocytes. *J. Biol. Chem.* 267:7963–7966.

Finch, E. A., and S. M. Goldin. 1994. Calcium and inositol 1,4,5-trisphosphate-induced Ca^{2+} release (response). *Science.* 265:813–814.

Finch, E. A., T. J. Turner, and S. M. Goldin. 1991. Calcium as a coagonist of inositol 1,4,5-trisphosphate-induced calcium release. *Science.* 252: 443–446.

Gilkey, J. C., L. F. Jaffe, E. B. Ridgway, and G. T. Reynolds. 1978. A free calcium wave traverses the activating egg of the medaka, *Oryzias latipes. J. Cell Biol.* 76:448–466.

Girard, S., and D. Clapham. 1992. Acceleration of intracellular calcium waves in *Xenopus* oocytes by calcium influx. *Science.* 260:229–232.

Grynkiewicz, G., M. Poenie, and R. Y. Tsien. 1985. A new generation of calcium indicators with greatly improved fluorescent properties. *J. Biol. Chem.* 260:3440–3450.

Guerrero, A., J. J. Singer, and F. S. Fay. 1994. Simultaneous measurements of Ca^{2+} release and influx into smooth muscle cells in response to caffeine. *J. Gen. Physiol.* 104:395–422.

Hodgkin, A. L., and R. D. Keynes. 1957. Movements of labelled calcium in squid giant axons. *J. Physiol.* 138:253–281.

Iino, M. 1990. Biphasic Ca^{2+} dependence of inositol 1,4,5-trisphosphate-induced Ca^{2+} release in smooth muscle cells of the guinea pig taenia caeci. *J. Gen. Physiol.* 95:1103–1122.

Iino, M., and M. Endo. 1992. Calcium-dependent immediate feedback control of inositol 1,4,5-trisphosphate-induced Ca^{2+} release. *Nature.* 360:76–78.

Inoué, S. 1986. Video Microscopy. Plenum Press, New York. 584 pp.

Irving, M., J. Maylie, N. L. Sizto, and W. K. Chandler. 1990. Intracellular diffusion in the presence of mobile buffers: application to proton movement in muscle. *Biophys. J.* 57:717–721.

Jaffe, L. F. 1983. Sources of calcium in egg activation: a review and hypothesis. *Dev. Biol.* 99:265–76.

Jaffe, L. F. 1991. The path of calcium in cytosolic calcium oscillations: a unifying hypothesis. *Proc. Natl. Acad. Sci. USA.* 88:9883–9887.

Kao, J. P. Y., and R. Y. Tsien. 1988. Ca^{2+} binding kinetics of fura-2 and azo-1 from temperature-jump relaxation measurements. *Biophys. J.* 53: 635–639.

Kasai, H., and G. J. Augustine. 1990. Cytosolic Ca^{2+} gradients triggering unidirectional fluid secretion from exocrine pancreas. *Nature.* 348:735–738.

Keener, J. P., and J. J. Tyson. 1986. Spiral waves in the Belousov-Zhabotinskii reaction. *Physica.* 21D:307–324.

Kimhi, Y., C. Palfrey, I. Spector, Y. Barak, and U. Z. Littauer. 1976. Maturation of neuroblastoma cells in the presence of dimethylsulfoxide. *Proc. Natl. Acad. Sci. USA.* 73:462–466.

Lechleiter, J. D., and D. E. Clapham. 1992. Molecular mechanisms of intracellular calcium excitability in X. laevis oocytes. *Cell.* 69:283–294.

Lechleiter, J., S. Girard, E. Peralta, and D. Clapham. 1991. Spiral calcium wave propagation and annihilation in Xenopus laevis oocytes. *Science.* 253:123–126.

Luther, R. 1906. Translated by R. Arnold, K. Showalter, and J. J. Tyson. (1987) Propagation of chemical reactions in space. *J. Chem. Educ.* 64:740–742.

Mathes, C., and S. H. Thompson. 1994. Calcium current activated by muscarinic receptors and thapsigargin in neuronal cells. *J. Gen. Physiol.* 104:107–122.

Meyer, T. 1991. Cell signaling by second messenger waves. *Cell.* 64: 675–678.

Meyer, T., D. Holowka, and L. Stryer. 1988. Highly cooperative opening of calcium channels by inositol 1,4,5-trisphosphate. *Science.* 240: 653–656.

Neher, E. 1986. Concentration profiles of intracellular calcium in the presence of a diffusible chelator. *Exp. Brain Res.* Ser 14:80–96.

Neher, E., and G. J. Augustine. 1992. Calcium gradients and buffers in bovine chromaffin cells. *J. Physiol.* 450:273–301.

Oakes, S. G., P. A. Iaizzo, E. Richelson, and G. Powis. 1988. Histamine-induced intracellular free Ca^{++}, inositol phosphate and electrical changes in murine N1E-115 neuroblastoma cells. *J. Pharmacol. Exp. Ther.* 247:114–121.

Parker, I., and I. Ivorra. 1990. Localized all-or-none calcium liberation by inositol trisphosphate. *Science.* 250:977–979.

Pethig, R., M. Kuhn, R. Payne, E. Adler, T.-H. Chen, and L. F. Jaffe. 1989. On the dissociation constants of BAPTA-type calcium buffers. *Cell Calcium.* 10:491–498.

Pozzan, T., and R. Tsien. 1989. Measurement of cytosolic free Ca^{2+} with quin2. *Methods Enzymol.* 172:230–262.

Pusch, M. and E. Neher. 1988. Rates of diffusional exchange between small cells and a measuring patch pipette. *Pflügers Arch.* 411: 204–211.

Renard, D., J. Poggioli, B. Berthon, and M. Claret. 1987. How far does phospholipase C activity depend on the cell calcium concentration? A study in intact cells. *Biochem. J.* 243:391–398.

Rhee, S. G., P.-G. Suh, S.-H. Ryu, and S. Y. Lee. 1989. Studies of inositol phospholipid-specific phospholipase C. *Science.* 244:546–550.

Richardson, A., and C. W. Taylor. 1993. Effects of Ca^{2+} chelators on purified inositol 1,4,5-trisphosphate ($InsP_3$) receptors and $InsP_3$-stimulated Ca^{2+} mobilization. *J. Biol. Chem.* 268:11528–11533.

Robinson, R. A., and R. H. Stokes. 1955. Electrolyte Solutions. Butterworths, London.

Seamon, K. B., and R. H. Kretsinger. 1983. Calcium-modulated proteins. *In* Calcium in Biology. T. G. Spiro, editor. (Metals in Biology, vol. 6). Wiley and Sons, New York. 1–52.

Smith, S. J., and G. J. Augustine. 1988. Calcium ions, active zones and synaptic transmitter release. *Trends Neurosci.* 11:458–464.

Sneyd, J., and L. V. Kalachev. 1994. A profile analysis of propagating calcium waves. *Cell Calcium.* 15:289–296.

Spät, A., P. G. Bradford, J. S. McKinney, R. P. Rubin, and J. W. Putney Jr. 1986. A saturable receptor for ^{32}P-inositol-1,4,5-trisphosphate in hepatocytes and neutrophils. *Nature.* 319:514–516.

Stern, M. D. 1992. Buffering of calcium in the vicinity of a channel pore. *Cell Calcium.* 13:183–192.

Surichamorn, W., C. Forray, and E. E. El-Fakahany 1990. Role of intracellular Ca^{2+} mobilization in muscarinic and histamine receptor-mediated activation of guanylate cyclase in N1E-115 neuroblastoma cells: assessment of the arachidonic acid release hypothesis. *Mol. Pharmacol.* 37:860–869.

Tank, D. W., W. G. Regehr, and K. R. Delaney. 1991. Modeling a synaptic chemical computation: the buildup and decay of presynaptic calcium. *Soc. Neurosci. Abst.* 231.13.

Timmerman, M. P., and C. C. Ashley. 1986. Fura-2 diffusion and its use as an indicator of transient free calcium changes in single striated muscle cells. *FEBS Lett.* 209:1–7.

Toescu, E. C., A. K. Lawrie, D. V. Gallacher, and O. H. Petersen. 1993. The pattern of agonist-evoked cytosolic Ca^{2+} oscillations depends on the resting intracellular Ca^{2+} concentration. *J. Biol. Chem.* 268: 18654–18658.

Tse, A., F. W. Tse, and B. Hille. 1994. Calcium homeostasis in identified rat gonadotrophs. *J. Physiol.* 477:511–525.

Tsien, R. Y. 1980. New calcium indicators and buffers with high selectivity against magnesium and protons: design, synthesis, and properties of prototype structures. *Biochemistry.* 19:2396–2404.

Tyson, J. J., and Keener, J. P. 1988. Singular perturbation theory of traveling waves in excitable media (a review). *Physica.* D32:327–361.

Wagner, J., and J. Keizer. 1994. Effects of rapid buffers on Ca^{2+} diffusion and Ca^{2+} oscillations. *Biophys. J.* 67:447–456.

Wang, S. S.-H. 1994. The initiation and propagation of calcium waves in neuronal cells. Stanford University, Ph. D. dissertation.

Wang, S. S.-H., A. A. Alousi, and S. H. Thompson. 1995. The lifetime of inositol 1,4,5-trisphosphate in single cells. *J. Gen. Physiol.* 105:149–171.

Wang, S. S.-H., and S. H. Thompson. 1994. Measurement of changes in muscarinic and histaminergic receptor density in single neuroblastoma cells using calcium release desensitization. *Cell Calcium.* 15:483–496.

Winfree, A. T. 1987. When Time Breaks Down: The Three-Dimensional Dynamics of Electrochemical Waves and Cardiac Arrythmias. Princeton University Press, New Jersey. 340 pp.

Yao, Y., and I. Parker. 1992. Potentiation of inositol trisphosphate-induced Ca^{2+} mobilization in *Xenopus* oocytes by cytosolic Ca^{2+}. *J. Physiol.* 458:319–338.

Yuste, R., A. Peinado, and L. C. Katz. 1992. Neuronal domains in developing neocortex. *Science.* 257:665–669.

Zhou, Z., and E. Neher. 1993. Mobile and immobile calcium buffers in bovine adrenal chromaffin cells. *J. Physiol.* 469:245–273.